Design and optimization of broadband wide-angle antireflection structures for binary diffractive optics

Chih-Hao Chang,[1,2,*] Laura Waller,[3] and George Barbastathis[1,2]

[1]*Singapore-MIT Alliance for Research and Technology (SMART) Centre, Singapore*
[2]*Department of Mechanical Engineering, Massachusetts Institute of Technology, Cambridge, Massachusetts 02139, USA*
[3]*Department of Electrical Engineering and Computer Science, Massachusetts Institute of Technology, Cambridge, Massachusetts 02139, USA*
**Corresponding author: chichang@smart.mit.edu*

Received December 7, 2009; revised February 4, 2010; accepted February 12, 2010; posted February 26, 2010 (Doc. ID 120960); published March 18, 2010

We propose a class of antireflecting structures that can effectively suppress reflections for binary diffractive optics. In this structure, multiple periodic thin films with gradually varying refractive indices are used to shift all reflected diffraction to the transmitted orders. The structure is optimized to operate over broad bands and wide angles using rigorous coupled-wave analysis and genetic algorithms. We validated the structure numerically using finite-difference time-domain methods. The proposed structure may lead to more efficient diffractive devices for applications in thin-film photovoltaic, waveguide coupler, and holographic optical elements. © 2010 Optical Society of America

OCIS codes: 050.1950, 050.1380, 310.1210.

In recent years there has been significant interest in the development of broadband, omnidirectional antireflective (AR) surfaces by using structures with gradually varying index of refraction. These structures employ a gradient index profile to suppress Fresnel reflections that typically result owing to the index mismatch between optical interfaces [1,2]. Such AR structures can be fabricated using lithographically defined subwavelength nanostructures [3,4], deposition of multilayer porous films [5,6], plasma etching to form randomly positioned nanoscale tips [7], and self-assembly of subwavelength colloidal nanospheres [8]. All these methods can achieve an effective index profile that is gradually varying, effectively preventing losses from Fresnel reflections.

Diffractive optics, such as gratings, Fresnel zone plates, and holograms, also suffer losses from Fresnel reflections as a result of index mismatch. These unwanted losses take the form of reflected diffraction orders. Recent work by Elfström *et al.* has demonstrated that placing an AR layer under a grating can effectively reduce such reflections for a given wavelength and a short range of angles [9]. In this Letter we propose an alternative class of AR structures for binary diffractive optics that consists of multilayer, periodic gradient-index films. The proposed structure is optimized and numerically demonstrated to suppress all reflected orders over broad bands and wide angles. Such a structure can be fabricated by modifying existing techniques developed for gradient-index AR surfaces and may be useful for creating more efficient photovoltaic cells [10,11] and waveguide couplers [12] based on diffractive optics.

The proposed AR structure for a binary grating is depicted in Fig. 1(a). The rectangular grating with period Λ and grating depth d_g has multilayer periodic thin-film stacks on both the ridge and groove regions, whose main functionality is to transfer all the reflected energy to the transmitted orders. A more detailed illustration of the AR structure is shown in Fig. 1(b), where the multilayer has N layers and the ith layer has index n_i and thickness d_i. The refractive indices are chosen so that $n_{air} < n_i < n_s$, and n_i increases gradually as i goes from 1 to N. The duty cycle of the grating is given by g and the substrate index is n_s. In this stack configuration the periodic index modulation in x increases gradually through each plane in z. This effect is analogous to stratified AR surfaces, except in our case the stratification follows the grating surface profile.

To analyze the proposed AR structure we simulated its diffraction efficiencies using rigorous coupled-wave analysis (RCWA) [13,14]. The first structure studied has $\Lambda = 2000$ nm, $d_g = 1000$ nm, $g = 0.5$, and a substrate index of 1.8 chosen for a heavy glass mate-

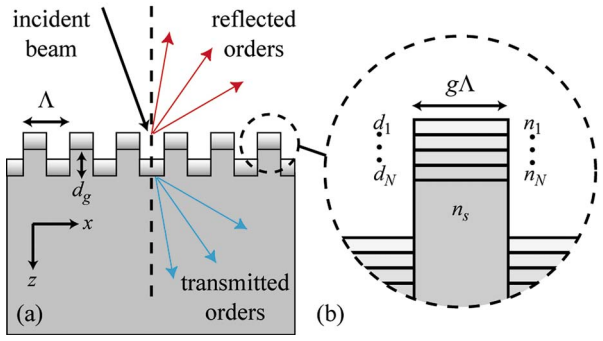

Fig. 1. (Color online) (a) Schematic of the proposed AR structure for a binary grating. (b) The structure consists of multilayers of periodic thin films with gradually varying refractive index on both the ridge and the groove of the grating.

rial. The incident light has $\lambda = 633$ nm and an incident angle of 0° and is TE polarized. The AR structure consists of $N = 7$ layers, n_i increasing linearly from 1.1 to 1.7 (1.1, 1.2,..., 1.7), and constant thickness d_o for each layer. The reflected and transmitted diffraction efficiencies are simulated for varying d_o, as shown in Fig. 2. The suppression of all reflected orders is observed as d_o increases from 0 to 60 nm, while the total reflection decreases from ~8% for a bare grating to ~0.1% at $d_o = 60$ nm. The transmitted efficiencies are in turn enhanced, as the total transmitted efficiency increases to near 100%. A similar effect can be seen for TM-polarized light, decreasing the total reflection from ~5% to ~0.07%.

The total reflected efficiency can be further suppressed by optimizing the thicknesses of each AR layer using genetic algorithms. The fitness function is chosen to have N thickness parameters in the search space and is given by

$$f(d_i) = \sum_j R_j(d_i), \tag{1}$$

where R_j is the diffraction efficiency of the jth reflected order calculated by RCWA and $i = 1$ to N. Two different index profiles, the linear and a quintic profile [1,2] given by

$$n_i = n_{air} + (n_s - n_{air})\left[10\left(\frac{d_i}{N+1}\right)^3 - 15\left(\frac{d_i}{N+1}\right)^4 + 6\left(\frac{d_i}{N+1}\right)^5\right], \tag{2}$$

where $i = 1$ to N, were used in our model. The discretized index profiles are adapted from AR surfaces with continuous profiles [1,2]. The algorithm is run with a population size of 20 for 500 generations, using the previously described optical configuration.

The optimized total reflection for both linear and quintic index profiles are plotted with varying N, shown in Fig. 3. For $N = 0$, the case where no AR structure is used, the total reflection is ~8%, as illustrated in Fig. 2. For both profiles, the reflection is suppressed dramatically as the number of layers in the AR structure increases. The quintic profile is also shown to have better AR performance, especially at higher N. These results demonstrate that a less-complex AR structure with five layers is sufficient for suppressing the total reflection by 4 orders of magnitude. For example, for the quintic profile with $N = 5$ ($n_i = 1.03$, 1.17, 1.4, 1.63, and 1.77), the optimized thicknesses d_1 to d_5 are 175.7, 154, 137.1, 104.5, and 59.2 nm, respectively, yielding a total reflection efficiency of 9.5×10^{-6}. To examine the design tolerance, 10% thickness error and 0.02 index offset are added to all layers, and the total reflection increases to 5.7×10^{-5}. While roughly 5 times greater than the optimized solution, the reflectivity is still significantly reduced.

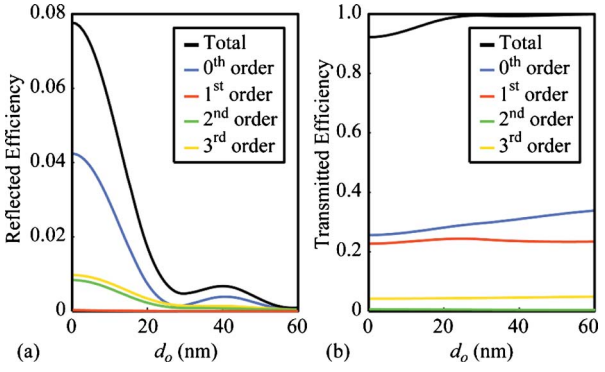

Fig. 2. (Color online) Simulated (a) reflected and (b) transmitted diffraction efficiencies for varying individual film thickness d_o in an $N = 7$ AR structure.

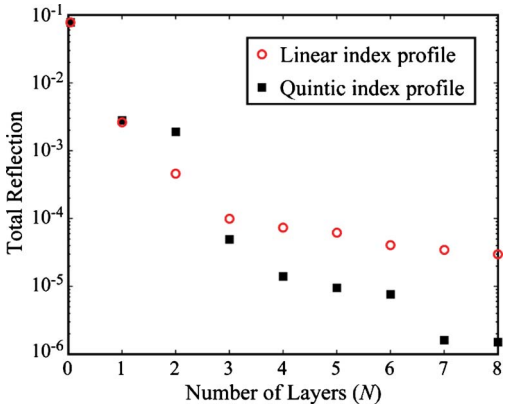

Fig. 3. (Color online) Optimized total reflection for varying the number of layers N in the AR structure.

We used finite-difference time-domain (FDTD) methods to numerically validate the optimized AR structure, illustrated in Fig. 4. Using a commercially available FDTD package from Lumerical Solutions, we propagate a short pulse (~4 fs) of a TE-polarized plane wave with a center wavelength of $\lambda = 633$ nm along the z direction at normal incidence. The color scale denotes the normalized magnitude E_y captured at the instant shortly after the light diffracts from a binary grating without and with the optimized AR structure, as shown in Figs. 4(a) (Media 1) and 4(b) (Media 2), respectively. The AR structure is outlined, using the optimized parameters for $N = 5$ that were obtained using genetic algorithms. Significant reflec-

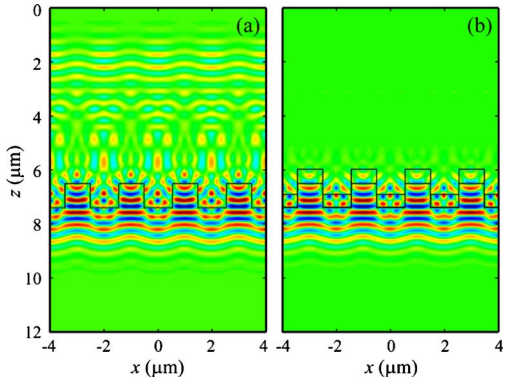

Fig. 4. (Color online) Reflection of a normal incident plane wave with $\lambda = 633$ nm from a binary diffraction grating (a) without (Media 1) and (b) with (Media 2) the optimized AR structure simulated using FDTD. The scale denotes normalized E_y fields.

tion from the grating can be observed for the case without the AR structure. On the contrary, the reflection is suppressed in the case where the optimized AR structure is used, and almost all of the light propagates into the grating. The total reflection is reduced by roughly 4 orders of magnitude. Note that, other than the reduced reflection, the field profiles are nearly identical.

So far the design of the AR structure has been focused on monochromatic light at normal incidence, but the proposed AR structure can also be used for broad bands and large angles. The fitness function used is

$$f(d_i) = \sum_l \sum_k \sum_j R_{jkl}(d_i), \tag{3}$$

where $\lambda_k = 400$ to 1000 nm at 100 nm step and $\theta_l = 0$ to 60° at 10° steps. For a quintic profile with $N = 5$, the optimized AR structure has thicknesses d_1 to d_5, equal to 155.8, 127.8, 106.3, 90.5, 91.4 nm, respectively.

The broadband effect of the AR structure can be observed in Fig. 5(a), where the reflected efficiencies are plotted for a grating with and without the AR coating. The plots were simulated at normal incidence. Both TE and TM polarizations show a reduction in total reflection by roughly 3 orders of magnitude for $\lambda = 400-1000$ nm. The angular dependence of reflected efficiency is illustrated in Fig. 5(b) for incident wavelength $\lambda = 633$ nm. The AR structure is able

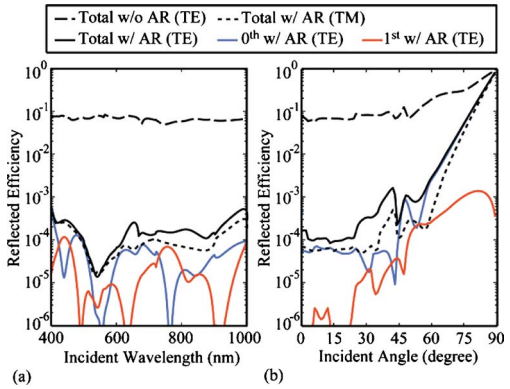

Fig. 5. (Color online) Simulated reflected diffraction efficiencies using RCWA for the optimized broadband wide-angle AR structure as functions of (a) wavelength for normal incidence and (b) incident angle for $\lambda = 633$ nm. Higher-order diffraction efficiencies are not shown.

to reduce the total reflection to below 1% at angles as large as 66° for both TE and TM polarizations, improvements of up to 3 orders of magnitude.

In our current design the AR structure consists of multilayer films; however, it is also possible to implement subwavelength nanostructures to achieve the same effect. From a fabrication perspective tapered nanostructures may be more feasible, since film coating over topography can be problematic and thus limited to gratings with large periods. In either case, superior diffractive performance can be achieved using the proposed AR structure with fabrication processes that are well understood.

This research was funded by the Singapore National Research Foundation (NRF) through the Singapore-MIT Alliance for Research and Technology (SMART) Centre, Center for Environmental Sensing and Monitoring (CENSAM).

References

1. W. H. Southwell, Opt. Lett. **8**, 584 (1983).
2. E. B. Grann, M. G. Moharam, and D. A. Pommet, J. Opt. Soc. Am. A **12**, 333 (1995).
3. P. Lalanne and G. M. Morris, Nanotechnology **8**, 53 (1997).
4. Y. Kanamori, M. Sasaki, and K. Hane, Opt. Lett. **24**, 1422 (1999).
5. J.-Q. Xi, M. F. Schubert, J. K. Kim, E. F. Schubert, M. Chen, S.-Y. Lin, W. Liu, and J. A. Smart, Nature Photon. **1**, 176 (2007).
6. M.-L. Kuo, D. J. Poxson, Y. S. Kim, F. W. Mont, J. K. Kim, E. F. Schubert, and S.-Y. Lin, Opt. Lett. **33**, 2527 (2008).
7. Y.-F. Huang, S. Chattopadhyay, Y.-J. Jen, C.-Y. Peng, T.-A. Liu, Y.-K. Hsu, C.-L. Pan, H.-C. Lo, C.-H. Hsu, Y.-H. Chang, C.-S. Lee, K.-H. Chen, and L.-C. Chen, Nature Nanotechnol. **2**, 770 (2007).
8. Y. Zhao, J. Wang, and G. Mao, Opt. Lett. **30**, 1885 (2005).
9. H. Elfström, T. Vallius, M. Kuittinen, J. Turunen, T. Clausnitzer, and E.-B. Kley, Opt. Express **12**, 6385 (2004).
10. H. Stiebig, N. Senoussaoui, C. Zahren, C. Haase, and J. Müller, Prog. Photovoltaics **14**, 13 (2006).
11. C. Eisele, C. E. Nebel, and M. Stutzmann, J. Appl. Phys. **89**, 7722 (2001).
12. D. Taillaert, P. Bienstman, and R. Baets, Opt. Lett. **29**, 2749 (2004).
13. M. G. Moharam, E. B. Grann, D. A. Pommet, and T. K. Gaylord, J. Opt. Soc. Am. A **12**, 1068 (1995).
14. M. G. Moharam, D. A. Pommet, E. B. Grann, and T. K. Gaylord, J. Opt. Soc. Am. A **12**, 1077 (1995).